

Chapter 2

Basic Theory of Cavity Optomechanics

Aashish A. Clerk and Florian Marquardt

Abstract This chapter provides a brief basic introduction to the theory used to describe cavity-optomechanical systems. This can serve as background information to understand the other chapters of the book. We first review the Hamiltonian and show how it can be approximately brought into quadratic form. Then we discuss the classical dynamics both in the linear regime (featuring optomechanical damping, optical spring, strong coupling, and optomechanically induced transparency) and in the nonlinear regime (optomechanical self-oscillations and attractor diagram). Finally, we discuss the quantum theory of optomechanical cooling, using the powerful and versatile quantum noise approach.

2.1 The Optomechanical Hamiltonian

Cavity optomechanical systems display a parametric coupling between the mechanical displacement \hat{x} of a mechanical vibration mode and the energy stored inside a radiation mode. That is, the frequency of the radiation mode depends on \hat{x} and can be written in the form $\omega_{\text{opt}}(\hat{x})$. When this dependence is Taylor-expanded, it is usually sufficient to keep the linear term, and we obtain the basic cavity-optomechanical Hamiltonian

$$\hat{H}_0 = \hbar (\omega_{\text{opt}}(0) - G\hat{x}) \hat{a}^\dagger \hat{a} + \hbar \Omega_M \hat{b}^\dagger \hat{b} + \dots \quad (2.1)$$

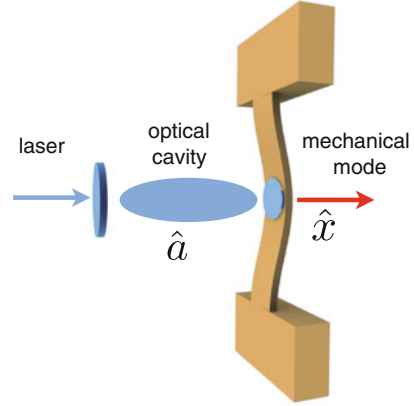
A. A. Clerk (✉)

Department of Physics, McGill University, Montreal, Canada
e-mail: clerk@physics.mcgill.ca

F. Marquardt

Institute for Theoretical Physics, Universität Erlangen-Nürnberg, Erlangen, Germany
e-mail: Florian.Marquardt@fau.de

Fig. 2.1 A typical system in cavity optomechanics consists of a laser-driven optical cavity whose light field exerts a radiation pressure force on a vibrating mechanical resonator



We have used Ω_M to denote the mechanical frequency, $\hat{a}^\dagger \hat{a}$ is the number of photons circulating inside the optical cavity mode, and $\hat{b}^\dagger \hat{b}$ is the number of phonons inside the mechanical mode of interest. Here G is the optomechanical frequency shift per displacement, sometimes also called the “frequency pull parameter”, that characterizes the particular system. For a simple Fabry–Perot cavity with an oscillating end-mirror (illustrated in Fig. 2.1), one easily finds $G = \omega_{\text{opt}}/L$, where L is the length of the cavity. This already indicates that smaller cavities yield larger coupling strengths. A detailed derivation of this Hamiltonian for a model of a wave field inside a cavity with a moving mirror can be found in [1]. However, the Hamiltonian is far more general than this derivation (for a particular system) might suggest: Whenever mechanical vibrations alter an optical cavity by leading to distortions of the boundary conditions or changes of the refractive index, we expect a coupling of the type shown here. The only important generalization involves the treatment of more than just a single mechanical and optical mode (see the remarks below).

A coupling of the type shown here is called ‘dispersive’ (in contrast to a ‘dissipative’ coupling, which would make κ depend on the displacement). Note that we have left out the terms responsible for the laser driving and the decay (of photons and of phonons), which will be dealt with separately in the following.

From this Hamiltonian, it follows that the radiation pressure force is

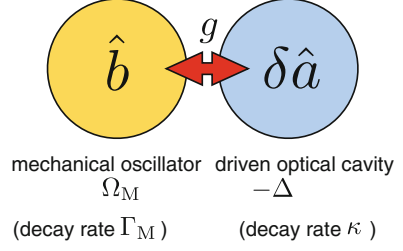
$$\hat{F}_{\text{rad}} = \hbar G \hat{a}^\dagger \hat{a}. \quad (2.2)$$

After switching to a frame rotating at the incoming laser frequency ω_L , we introduce the detuning $\Delta = \omega_L - \omega_{\text{opt}}(0)$, such that we get

$$\hat{H} = -\hbar \Delta \hat{a}^\dagger \hat{a} - \hbar G \hat{x} \hat{a}^\dagger \hat{a} + \hbar \Omega_M \hat{b}^\dagger \hat{b} + \dots \quad (2.3)$$

It is now possible to write the displacement $\hat{x} = x_{\text{ZPF}}(\hat{b} + \hat{b}^\dagger)$ in terms of the phonon creation and annihilation operators, where $x_{\text{ZPF}} = (\hbar/2m_{\text{eff}}\Omega_M)^{1/2}$ is the size of the

Fig. 2.2 After linearization, the standard system in cavity optomechanics represents two coupled harmonic oscillators, one of them mechanical (at a frequency Ω_M), the other optical (at an effective frequency given by the negative detuning $-\Delta = \omega_{\text{opt}}(0) - \omega_L$)



mechanical ground state wave function (“mechanical zero-point fluctuations”). This leads to

$$\hat{H} = -\hbar\Delta\hat{a}^\dagger\hat{a} - \hbar g_0 \left(\hat{b} + \hat{b}^\dagger \right) \hat{a}^\dagger\hat{a} + \hbar\Omega_M\hat{b}^\dagger\hat{b} + \dots \quad (2.4)$$

Here $g_0 = Gx_{\text{ZPF}}$ represents the coupling between a single photon and a single phonon. Usually g_0 is a rather small frequency, much smaller than the cavity decay rate κ or the mechanical frequency Ω_M . However, the effective photon-phonon coupling can be boosted by increasing the laser drive, at the expense of introducing a coupling that is only quadratic (instead of cubic as in the original Hamiltonian). To see this, we set $\hat{a} = \alpha + \delta\hat{a}$, where α is the average light field amplitude produced by the laser drive (i.e. $\alpha = \langle \hat{a} \rangle$ in the absence of optomechanical coupling), and $\delta\hat{a}$ represents the small quantum fluctuations around that constant amplitude. If we insert this into the Hamiltonian and only keep the terms that are linear in α , we obtain

$$\hat{H}_{(\text{lin})} = -\hbar\Delta\delta\hat{a}^\dagger\delta\hat{a} - \hbar g \left(\hat{b} + \hat{b}^\dagger \right) \left(\delta\hat{a} + \delta\hat{a}^\dagger \right) + \hbar\Omega_M\hat{b}^\dagger\hat{b} + \dots \quad (2.5)$$

This is the so-called “linearized” optomechanical Hamiltonian (where the equations of motion for $\delta\hat{a}$ and \hat{b} are in fact linear). Here $g = g_0\alpha$ is the enhanced, laser-tunable optomechanical coupling strength, and for simplicity we have assumed α to be real-valued (otherwise a simple unitary transformation acting on $\delta\hat{a}$ can bring the Hamiltonian to the present form, which is always possible unless two laser-drives are involved). We have thus arrived at a rather simple system: two coupled harmonic oscillators (Fig. 2.2).

Note that we have omitted the term $-\hbar g_0 |\alpha|^2 (\hat{b} + \hat{b}^\dagger)$, which represents a constant radiation pressure force acting on the mechanical resonator and would lead to a shift of the resonator’s equilibrium position. We can imagine (as is usually done in these cases), that this shift has already been taken care of and \hat{x} is measured from the new equilibrium position, or that this leads to a slightly changed “effective detuning” $\tilde{\Delta}$ (which will be the notation we use further below when solving the classical equations of motion). In addition, we have neglected the term $-\hbar g_0 \delta\hat{a}^\dagger \delta\hat{a} (\hat{b} + \hat{b}^\dagger)$, under the assumption that this term is “small”. The question when exactly this term may start to matter and lead to observable consequences is a subject of ongoing research (it seems that generally speaking $g_0/\kappa > 1$ is required).

As will be explained below, almost all of the elementary properties of cavity-optomechanical systems can be explained in terms of the linearized Hamiltonian.

Of course, the Hamiltonian in Eq. (2.1) represents an approximation (usually, an extremely good one). In particular, we have omitted all the other mechanical normal modes and all the other radiation modes. The justification for omitting the other optical modes would be that only one mode is driven (nearly) resonantly by the laser. With regard to the mechanical mode, optomechanical cooling or amplification in the resolved-sideband regime ($\kappa < \Omega_M$) usually affects only one mode, again selected by the laser frequency. Nevertheless, these simplistic arguments can fail, e.g. when κ is larger than the spacing between mechanical modes, when the distance between two optical modes matches a mechanical frequency, or when the dynamics becomes nonlinear, with large amplitudes of mechanical oscillations.

Cases where the other modes become important display an even richer dynamics than the one we are going to investigate below for the standard system (one mechanical mode, one radiation mode). Interesting experimental examples for the case of two optical modes and one mechanical mode can be found in the chapter by Bahl and Carmon (on Brillouin optomechanics), and in the contribution by Jack Sankey (on the membrane-in-the-middle setup).

In the following sections, we give a brief, self-contained overview of the most important basic features of this system, both in the classical regime and in the quantum regime. A more detailed introduction to the basics of the theory of cavity optomechanics can also be found in the recent review [2].

2.2 Classical Dynamics

The most important properties of optomechanical systems can be understood already in the classical regime. As far as current experiments are concerned, the only significant exception would be the quantum limit to cooling, which will be treated further below in the sections on the basics of quantum optomechanics.

2.2.1 Equations of Motion

In the classical regime, we assume both the mechanical oscillation amplitudes and the optical amplitudes to be large, i.e. the system contains many photons and phonons. As a matter of fact, much of what we will say is also valid in the regime of small amplitudes, when only a few photons and phonons are present. This is because in that regime the equations of motion can be linearized, and the expectation values of a quantum system evolving according to linear Heisenberg equations of motion in fact follow precisely the classical dynamics. The only aspect missing from the classical description in the linearized regime is the proper treatment of the quantum Langevin noise force, which is responsible for the quantum limit to cooling mentioned above.

We write down the classical equations for the position $x(t)$ and for the complex light field amplitude $\alpha(t)$ (normalized such that $|\alpha|^2$ would be the photon number in the semiclassical regime):

$$\ddot{x} = -\Omega_M^2(x - x_0) - \Gamma_M \dot{x} + (F_{\text{rad}} + F_{\text{ext}}(t))/m_{\text{eff}} \quad (2.6)$$

$$\dot{\alpha} = [i(\Delta + Gx) - \kappa/2]\alpha + \frac{\kappa}{2}\alpha_{\text{max}} \quad (2.7)$$

Here $F_{\text{rad}} = \hbar G |\alpha|^2$ is the radiation pressure force. The laser amplitude enters the term α_{max} in the second equation, where we have chosen a notation such that $\alpha = \alpha_{\text{max}}$ on resonance ($\Delta = 0$) in the absence of the optomechanical interaction ($G = 0$). Note that the dependence on \hbar in this equations vanishes once we express the photon number in terms of the total light energy \mathcal{E} stored inside the cavity: $|\alpha|^2 = \mathcal{E}/\hbar\omega_L$. This confirms that we are dealing with a completely classical problem, in which \hbar will not enter any end-results if they are expressed in terms of classical quantities like cavity and laser frequency, cavity length, stored light energy (or laser input power), cavity decay rate, mechanical decay rate, and mechanical frequency. Still, we keep the present notation in order to facilitate later comparison with the quantum expressions.

2.2.2 Linear Response of an Optomechanical System

We have also added an external driving force $F_{\text{ext}}(t)$ to the equation of motion for $x(t)$. This is because our goal now will be to evaluate the linear response of the mechanical system to this force. The idea is that the linear response will display a mechanical resonance that turns out to be modified due to the interaction with the light field. It will be shifted in frequency (“optical spring effect”) and its width will be changed (“optomechanical damping or amplification”). These are the two most important elementary effects of the optomechanical interaction. Optomechanical effects on the damping rate and on the effective spring constant have been first analyzed and observed (in a macroscopic microwave setup) by Braginsky and co-workers already at the end of the 1960s [3].

First one has to find the static equilibrium position, by setting $\dot{x} = 0$ and $\dot{\alpha} = 0$ and solving the resulting set of coupled nonlinear algebraic equations. If the light intensity is large, there can be more than one stable solution. This ‘static bistability’ was already observed in the pioneering experiment on optomechanics with optical forces by the Walther group in the 1980s [4]. We now assume that such a solution has been found, and we linearize around it: $x(t) = \bar{x} + \delta x(t)$ and $\alpha(t) = \bar{\alpha} + \delta\alpha(t)$. Then the equations for δx and $\delta\alpha$ read:

$$\delta\ddot{x}(t) = -\Omega_M^2\delta x - \Gamma_M\delta\dot{x} + \frac{\hbar G}{m_{\text{eff}}} [\bar{\alpha}^*\delta\alpha + \bar{\alpha}\delta\alpha^*] + \frac{F_{\text{ext}}(t)}{m_{\text{eff}}} \quad (2.8)$$

$$\delta\dot{\alpha}(t) = [i\bar{\Delta} - \kappa/2]\delta\alpha + iG\bar{\alpha}\delta x \quad (2.9)$$

Note that we have introduced the effective detuning $\bar{\Delta} = \Delta + G\bar{x}$, shifted due to the static mechanical displacement (this is often not made explicit in discussions of optomechanical systems, although it can become important for larger displacements). We are facing a linear set of equations, which in principle can be solved straightforwardly by going to Fourier space and inverting a matrix. There is only one slight difficulty involved here, which is that the equations also contain the complex conjugate $\delta\alpha^*(t)$. If we were to enter with an ansatz $\delta\alpha(t) \propto e^{-i\omega t}$, this automatically generates terms $\propto e^{+i\omega t}$ at the negative frequency as well. In some cases, this may be neglected (i.e. dropping the term $\delta\alpha^*$ from the equations), because the term $\delta\alpha^*(t)$ is not resonant (this is completely equivalent to the “rotating wave approximation” in the quantum treatment). However, here we want to display the full solution.

We now introduce the Fourier transform of any quantity $A(t)$ in the form $A[\omega] \equiv \int dt A(t) e^{i\omega t}$. Then, in calculating the response to a force given by $F_{\text{ext}}[\omega]$, we have to consider the fact that $(\delta\alpha^*)[\omega] = (\delta\alpha[-\omega])^*$. The equation for $\delta\alpha[\omega]$ is easily solved, yielding $\delta\alpha[\omega] = \chi_c(\omega) i G \bar{\alpha} \delta x[\omega]$, with $\chi_c(\omega) = [-i\omega - i\bar{\Delta} + \kappa/2]^{-1}$ the response function of the cavity. When we insert this into the equation for $\delta x[\omega]$, we exploit $(\delta\alpha^*)[\omega] = (\delta\alpha[-\omega])^*$ as well as $(\delta x[-\omega])^* = \delta x[\omega]$, since $\delta x(t)$ is real-valued. The result for the mechanical response is of the form

$$\delta x[\omega] = \frac{F_{\text{ext}}[\omega]}{m_{\text{eff}} (\Omega_M^2 - \omega^2 - i\omega\Gamma_M) + \Sigma(\omega)} \equiv \chi_{xx}(\omega) F_{\text{ext}}[\omega]. \quad (2.10)$$

Here we have combined all the terms that depend on the optomechanical interaction into the quantity $\Sigma(\omega)$ in the denominator. It is equal to

$$\Sigma(\omega) = -i\hbar G^2 |\bar{\alpha}|^2 [\chi_c(\omega) - \chi_c^*(-\omega)]. \quad (2.11)$$

Note that the prefactor can also be rewritten as $\hbar G^2 |\bar{\alpha}|^2 = 2m_{\text{eff}} \Omega_M g^2$, by inserting the expression for $x_{\text{ZPF}} = (\hbar/2m_{\text{eff}} \Omega_M)^{1/2}$ and using $(G x_{\text{ZPF}} |\bar{\alpha}|)^2 = g^2$.

One may call Σ the “optomechanical self-energy” [5]. This is in analogy to the self-energy of an electron appearing in the expression for its Green’s function, which summarizes the effects of the interaction with the electron’s environment (photons, phonons, other electrons, ...).

If the coupling is weak, the mechanical linear response will still have a single resonance, whose properties are just modified by the presence of the optomechanical interaction. In that case, close inspection of the denominator in Eq. (2.10) reveals the meaning of both the imaginary and the real part of Σ , which we evaluate at the original resonance frequency $\omega = \Omega$. The imaginary part describes some additional optomechanical damping, induced by the light field:

$$\begin{aligned} \Gamma_{\text{opt}} &= -\frac{1}{m_{\text{eff}} \Omega_M} \text{Im} \Sigma(\Omega) \\ &= g^2 \kappa \left\{ \frac{1}{(\Omega_M + \bar{\Delta})^2 + (\frac{\kappa}{2})^2} - \frac{1}{(\Omega_M - \bar{\Delta})^2 + (\frac{\kappa}{2})^2} \right\} \end{aligned} \quad (2.12)$$

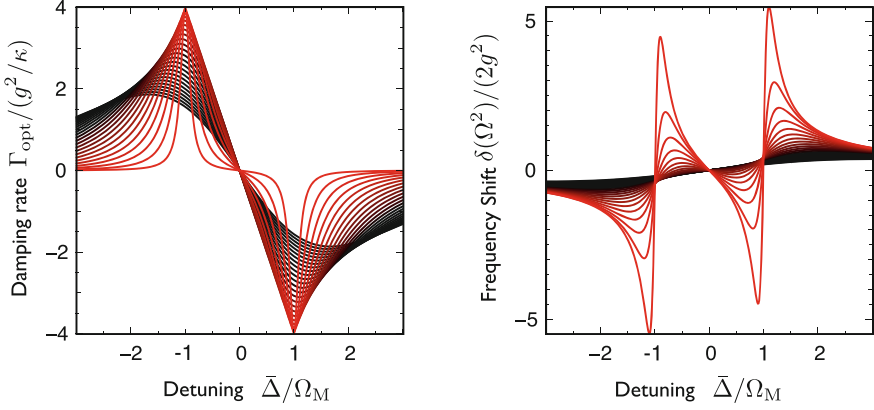


Fig. 2.3 Optomechanical damping rate (*left*) and frequency shift (*right*), as a function of the effective detuning $\bar{\Delta}$. The different curves depict the results for varying cavity decay rate, running in the interval $\kappa/\Omega_M = 0.2, 0.4, \dots, 5$ (the largest values are shown as *black lines*). We keep the intra-cavity energy fixed (i.e. g is fixed). Note that the damping rate Γ_{opt} has been rescaled by g^2/κ , which represents the parametric dependence of Γ_{opt} in the resolved-sideband regime $\kappa < \Omega_M$. In addition, note that we chose to plot the frequency shift in terms of $\delta(\Omega^2) \approx 2\Omega_M\delta\Omega$ (for small $\delta\Omega \ll \Omega_M$)

The real part describes a shift of the mechanical frequency (“optical spring”):

$$\begin{aligned} \delta(\Omega^2) &= \frac{1}{m_{\text{eff}}} \text{Re} \Sigma(\Omega) \\ &= 2\Omega_M g^2 \left\{ \frac{\Omega_M + \bar{\Delta}}{(\Omega_M + \bar{\Delta})^2 + (\frac{\kappa}{2})^2} - \frac{\Omega_M - \bar{\Delta}}{(\Omega_M - \bar{\Delta})^2 + (\frac{\kappa}{2})^2} \right\}. \end{aligned} \quad (2.13)$$

Both of these are displayed in Fig. 2.3. They are the results of “dynamical backaction”, where the (possibly retarded) response of the cavity to the mechanical motion acts back on this motion.

2.2.3 Strong Coupling Regime

When the optomechanical coupling rate g becomes comparable to the cavity damping rate κ , the system enters the strong coupling regime. The hallmark of this regime is the appearance (for red detuning) of a clearly resolved double-peak structure in the mechanical (or optical) susceptibility. This peak splitting in the strong coupling regime was first predicted in [5], then analyzed further in [6] and finally observed experimentally for the first time in [7]. This comes about because the mechanical resonance and the (driven) cavity resonance hybridize, like any two coupled harmonic oscillators, with a splitting $2g$ set by the coupling. In order to describe this correctly, we have to retain the full structure of the mechanical susceptibility, Eq. (2.10) at all

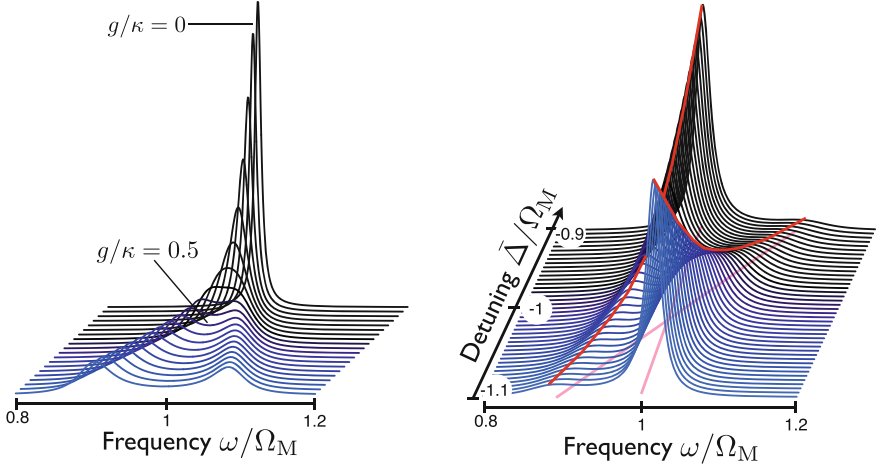


Fig. 2.4 Optomechanical strong coupling regime, illustrated in terms of the mechanical susceptibility. The figures show the imaginary part of $\chi_{xx}(\omega) = 1/(m(\Omega^2 - \omega^2 - i\omega\Gamma) + \Sigma(\omega))$. *Left* $\text{Im}\chi_{xx}(\omega)$ as a function of varying coupling strength g , set by the laser drive, for *red* detuning on resonance, $\bar{\Delta} = -\Omega$. A clear splitting develops around $g/\kappa = 0.5$. *Right* $\text{Im}\chi_{xx}(\omega)$ as a function of varying detuning $\bar{\Delta}$ between the laser drive and the cavity resonance, for fixed $g/\kappa = 0.5$

frequencies, without applying the previous approximation of evaluating $\Sigma(\omega)$ in the vicinity of the resonance (Fig. 2.4).

2.2.4 Optomechanically Induced Transparency

We now turn to the cavity response to a weak additional probe beam, which can be treated in analogy to the mechanical response discussed above. However, an interesting new feature develops, due to the fact that usually $\Gamma \ll \kappa$. Even for $g \ll \kappa$, the cavity response shows a spectrally sharp feature due to the optomechanical interaction, and its width is given by $\Gamma = \Gamma_M + \Gamma_{\text{opt}}$. This phenomenon is called “optomechanically induced transparency” [8, 9].

We can obtain the modified cavity response by imagining that there is no mechanical force ($F_{\text{ext}} = 0$), but instead there is an additional weak laser drive, which enters as $\dots + \delta\alpha_L e^{-i\omega t}$ on the right-hand-side of Eq. (2.9). By solving the coupled set of equations, we arrive at a modified cavity response

$$\delta\alpha(t) = \chi_c^{\text{eff}}(\omega)\delta\alpha_L e^{-i\omega t}, \quad (2.14)$$

where we find

$$\chi_c^{\text{eff}}(\omega) = \chi_c(\omega) \cdot \left[1 + 2im_{\text{eff}}\Omega_M g^2 \chi_c(\omega) \chi_{xx}(\omega) \right]. \quad (2.15)$$

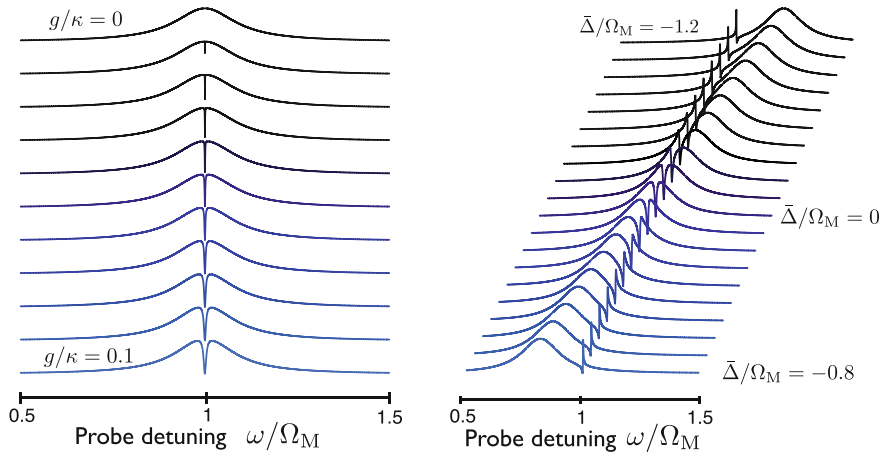


Fig. 2.5 Optomechanically induced transparency: Modification of the cavity response due to the interaction with the mechanical degree of freedom. We show $\text{Re}\chi_c^{\text{eff}}(\omega)$ as a function of the detuning ω between the weak probe beam and the strong(er) control beam, for variable coupling g of the control beam (*left*) and for variable detuning $\bar{\Delta}$ of the control beam versus the cavity resonance (*right*, at $g/\kappa = 0.1$). We have chosen $\kappa/\Omega_M = 0.2$. Note that in the *left* plot, for further increases in g , the curves shown here would smoothly evolve into the *double-peak* structure characteristic of the strong-coupling regime

Note that in the present section ω has the physical meaning of the detuning between the weak additional probe laser and the original (possibly strong) control beam at ω_L . That is: $\omega = \omega_{\text{probe}} - \omega_L$. The result is shown in Fig. 2.5. The sharp dip goes down to zero when $g^2/(\kappa \Gamma_M) \gg 1$. Ultimately, this result is an example of a very generic phenomenon: If two oscillators are coupled and they have very different damping rates, then driving the strongly damped oscillator (here: the cavity) can indirectly drive the weakly damped oscillator (here: the mechanics), leading to a sharp spectral feature on top of a broad resonance. In the context of atomic physics with three-level atoms, this has been observed as “electromagnetically induced transparency”, and thus the feature discussed here came to be called “optomechanically induced transparency”.

We note that for a blue-detuned control beam, the dip turns into a peak, signalling optomechanical amplification of incoming weak radiation.

2.2.5 Nonlinear Dynamics

On the blue-detuned side ($\bar{\Delta} > 0$), where Γ_{opt} is negative, the overall damping rate $\Gamma_M + \Gamma_{\text{opt}}$ diminishes upon increasing the laser intensity, until it finally becomes negative. Then the system becomes unstable and any small initial perturbation (e.g. thermal fluctuations) will increase exponentially at first, until the system settles into self-induced mechanical oscillations of a fixed amplitude: $x(t) = \bar{x} + A \cos(\Omega_M t)$. This is the optomechanical dynamical instability (parametric instability), which

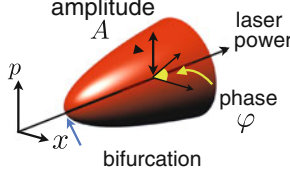


Fig. 2.6 When increasing a control parameter, such as the laser power, an optomechanical system can become unstable and settle into periodic mechanical oscillations. These correspond to a limit cycle in phase space of some amplitude A , as depicted here. The transition is called a Hopf bifurcation

has been explored both theoretically [10, 11] and observed experimentally in various settings (e.g. [12–14] for radiation-pressure driven setups and [15, 16] for photothermal light forces) (Fig. 2.6).

In order to understand the saturation of the amplitude A at a fixed finite value, we have to take into account that the mechanical oscillation changes the pattern of the light amplitude’s evolution. In turn, the overall effective damping rate, as averaged over an oscillation period, changes as well. To capture this, we now introduce an amplitude-dependent optomechanical damping rate. This can be done by noting that a fixed damping rate Γ would give rise to a power loss $\langle (m_{\text{eff}} \Gamma \dot{x}) \dot{x} \rangle = \Gamma m_{\text{eff}} A^2 / 2$. Thus, we define

$$\Gamma_{\text{opt}}(A) \equiv -\frac{2}{m_{\text{eff}} A^2} \langle F_{\text{rad}}(t) \dot{x}(t) \rangle. \quad (2.16)$$

This definition reproduces the damping rate Γ_{opt} calculated above in the limit $A \rightarrow 0$. The condition for the value of the amplitude on the limit cycle is then simply given by

$$\Gamma_{\text{opt}}(A) + \Gamma_{\text{M}} = 0. \quad (2.17)$$

The result for Eq. (2.16) can be expressed in terms of the exact analytical solution for the light field amplitude $\alpha(t)$ given the mechanical oscillations at amplitude A . This solution is a Fourier series, $|\alpha(t)| = \left| \frac{2\alpha_L}{\Omega_{\text{M}}} \sum_n \tilde{\alpha}_n e^{in\Omega_{\text{M}}t} \right|$, involving Bessel function coefficients. In the end, we find

$$\Gamma_{\text{opt}}(A) = 4 \left(\frac{\kappa}{\Omega_{\text{M}}} \right)^2 \frac{g^2}{\Omega_{\text{M}}} f \left(\frac{GA}{\Omega_{\text{M}}} \right), \quad (2.18)$$

where

$$f(a) = -\frac{1}{a} \sum_n \text{Im} \tilde{\alpha}_{n+1}^* \tilde{\alpha}_n \quad (2.19)$$

with

$$\tilde{\alpha}_n = \frac{1}{2} \frac{J_n(-a)}{in + \kappa / (2\Omega_{\text{M}}) - i\bar{\Delta} / \Omega_{\text{M}}}. \quad (2.20)$$

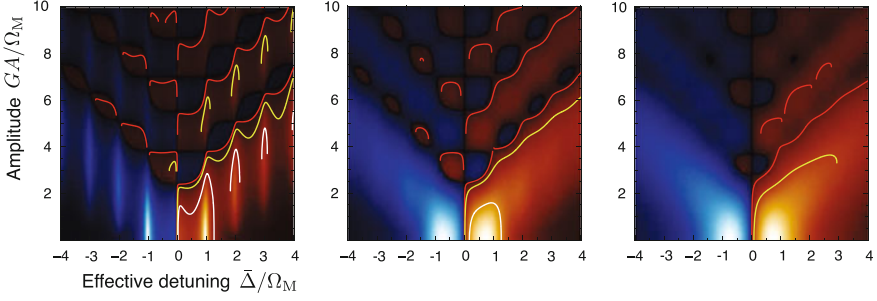


Fig. 2.7 Optomechanical Attractor Diagram: The effective amplitude-dependent optomechanical damping rate $\Gamma_{\text{opt}}(A)$, as a function of the oscillation amplitude A and the effective detuning $\bar{\Delta}$, for three different sidebands ratios $\kappa/\Omega_M = 0.2, 1, 2$, from left to right [Γ_{opt} in units of $\gamma_0 \equiv 4(\kappa/\Omega_M)^2 g^2/\Omega_M$, blue positive/cooling; red negative/amplification]. The optomechanical attractor diagram of self-induced oscillations is determined via the condition $\Gamma_{\text{opt}}(A) = -\Gamma_M$. The attractors are shown for three different values of the incoming laser power (as parametrized by the enhanced optomechanical coupling g at resonance), with $\Gamma_M/\gamma_0 = 0.1, 10^{-2}, 10^{-3}$ (white, yellow, red)

Note that g denotes the enhanced optomechanical coupling at resonance (i.e. for $\bar{\Delta} = 0$), i.e. it characterizes the laser amplitude. Also note that $\bar{\Delta}$ includes an amplitude-dependent shift due to a displacement of the mean oscillator position \bar{x} by the radiation pressure force $\langle F_{\text{rad}} \rangle$. This has to be found self-consistently.

The resulting attractor diagram is shown in Fig. 2.7. It shows the possible limit cycle amplitude(s) as a function of effective detuning $\bar{\Delta}$, such that the self-consistent evaluation of \bar{x} has been avoided.

The self-induced mechanical oscillations in an optomechanical system are analogous to the behaviour of a laser above threshold. In the optomechanical case, the energy provided by the incoming laser beam is converted, via the interaction, into coherent mechanical oscillations. While the amplitude of these oscillations is fixed, the phase depends on random initial conditions and may diffuse due to noise (e.g. thermal mechanical noise or shot noise from the laser). Interesting features may therefore arise when several such optomechanical oscillators are coupled, either mechanically or optically. In that case, they may synchronize if the coupling is strong enough. Optomechanical synchronization has been predicted theoretically [17, 18] and then observed experimentally [19, 20]. At high driving powers, we note that the dynamics is no longer a simple limit cycle but may instead become chaotic [21].

2.3 Quantum Theory

In the previous section, we have seen how a semiclassical description of the canonical optomechanical cavity gives a simple, intuitive picture of optical spring and optical damping effects. The average cavity photon number \bar{n}_{cav} acts as a force on

the mechanical resonator; this force depends on the mechanical position x , as changes in x change the cavity frequency and hence the effective detuning of the cavity drive laser. If \bar{n}_{cav} were able to respond instantaneously to changes in x , we would only have an optical spring effect; however, the fact that \bar{n}_{cav} responds to changes in x with a non-zero delay time implies that we also get an effective damping force from the cavity.

In this section, we go beyond the semiclassical description and develop the full quantum theory of our driven optomechanical system [5, 22, 23]. We will see that the semiclassical expressions derived above, while qualitatively useful, are not in general quantitatively correct. In addition, the quantum theory captures an important effect missed in the semiclassical description, namely the effective heating of the mechanical resonator arising from the fluctuations of the cavity photon number about its mean value. These fluctuations play a crucial role, in that they set a limit to the lowest possible temperature one can achieve via cavity cooling.

2.3.1 Basics of the Quantum Noise Approach to Cavity Backaction

We will focus here on the so-called “quantum noise” approach, where for a weak optomechanical coupling, one can understand the effects of the cavity backaction completely from the quantum noise spectral density of the radiation pressure force operator (Fig. 2.8). This spectral density is defined as:

$$S_{FF}[\omega] = \int_{-\infty}^{\infty} dt e^{i\omega t} \left\langle \hat{F}(t) \hat{F}(0) \right\rangle \quad (2.21)$$

where the average is taken over the state of the cavity at zero optomechanical coupling, and

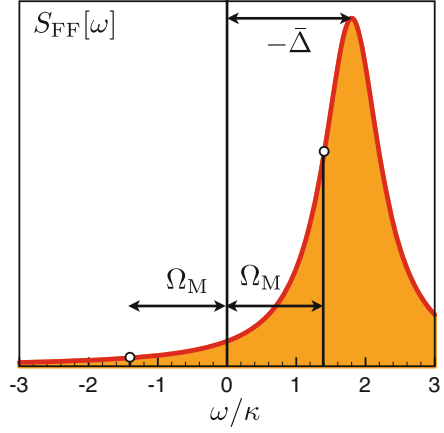
$$\hat{F}(t) \equiv \hbar G \left(\hat{a}^\dagger \hat{a} - \left\langle \hat{a}^\dagger \hat{a} \right\rangle \right) \quad (2.22)$$

is the noise part of the cavity’s backaction force operator (in the Heisenberg picture).

We start by considering the quantum origin of optomechanical damping, treating the optomechanical interaction term in the Hamiltonian of Eq. (2.3) using perturbation theory. Via the optomechanical interaction, the cavity will cause transitions between energy eigenstates of the mechanical oscillator, either upwards or downwards in energy. Working to lowest order in the optomechanical coupling G , these rates are described by Fermi’s Golden rule. A straightforward calculation (see Sect. II B of Ref. [24]) shows that the Fermi’s Golden rule rate $\Gamma_{n,+}$ ($\Gamma_{n,-}$) for a transition taking the oscillator from $n \rightarrow n+1$ quanta ($n \rightarrow n-1$ quanta) is given by:

$$\Gamma_{n,\pm} = \left(n + \frac{1}{2} \pm \frac{1}{2} \right) \frac{x_{\text{ZPF}}^2}{\hbar^2} S_{FF}[\mp \Omega_M] \quad (2.23)$$

Fig. 2.8 The noise spectrum of the radiation pressure force in a driven optical cavity. This is a Lorentzian, peaked at the (*negative*) effective detuning. The transition rates are proportional to the value of the spectrum at $+\Omega_M$ (emission of energy into the cavity bath) and at $-\Omega_M$ (absorption of energy by the mechanical resonator)



The optomechanical damping rate simply corresponds to the decay rate of the average oscillator energy due to these transitions. One finds (see Appendix B of Ref. [24]):

$$\Gamma_{\text{opt}} = \Gamma_{n,-} \left(\frac{1}{n} \right) - \Gamma_{n,+} \left(\frac{1}{(n+1)} \right) \quad (2.24)$$

$$= \frac{x_{\text{ZPF}}^2}{\hbar^2} (S_{FF}[\Omega_M] - S_{FF}[-\Omega_M]) \quad (2.25)$$

Note that one obtains simple linear damping (the damping is independent of the amplitude of the oscillator's motion). Also note that our derivation has neglected the effects of the oscillator's intrinsic damping Γ_M , and thus is only valid if Γ_M is sufficiently small; we comment more on this at the end of the section.

There is a second way to derive Eq. (2.25) which is slightly more general, and which allows us to calculate the optical spring constant k_{opt} ; it also more closely matches the heuristic reasoning that led to the semiclassical expressions of the previous section. We start from the basic fact that both Γ_{opt} and $\delta\Omega_{M,\text{opt}}$ arise from the dependence of the average backaction force F_{rad} on the mechanical position x . We can calculate this dependence to lowest order in G using the standard equations of quantum linear response (i.e. the Kubo formula):

$$\delta F_{\text{rad}}(t) = - \int_{-\infty}^{\infty} dt' \lambda_{FF}(t-t') \langle \hat{x}(t') \rangle \quad (2.26)$$

where the causal force-force susceptibility $\lambda_{FF}(t)$ is given by:

$$\lambda_{FF}(t) = -\frac{i}{\hbar} \theta(t) \left\langle \left[\hat{F}(t), \hat{F}(0) \right] \right\rangle \quad (2.27)$$

Next, assume that the oscillator is oscillating, and thus $\langle \hat{x}(t) \rangle = x_0 \cos \Omega_M t$. We then have:

$$\delta F_{\text{rad}}(t) = (-\text{Re } \lambda_{FF}[\Omega_M] \cdot x_0 \cos \Omega_M t) - (\text{Im } \lambda_{FF}[\Omega_M] \cdot x_0 \sin \Omega_M t) \quad (2.28)$$

$$= -\Delta k_{\text{opt}} \langle \hat{x}(t) \rangle - m_{\text{eff}} \Gamma_{\text{opt}} \left\langle \frac{d\hat{x}}{dt}(t) \right\rangle \quad (2.29)$$

Comparing the two lines above, we see immediately that the real and imaginary parts of the Fourier-transformed susceptibility $\lambda_{FF}[\Omega_M]$ are respectively proportional to the optical spring k_{opt} and the optomechanical damping Γ_{opt} . The susceptibility can in turn be related to $S_{FF}[\omega]$. In the case of the imaginary part of $\lambda_{FF}[\omega]$, a straightforward calculation yields:

$$-\text{Im } \lambda_{FF}[\omega] = \frac{S_{FF}[\omega] - S_{FF}[-\omega]}{2\hbar} \quad (2.30)$$

As a result, the definition of Γ_{opt} emerging from Eq. (2.29) is identical to that in Eq. (2.25). The real part of $\lambda_{FF}[\omega]$ can also be related to $S_{FF}[\omega]$ using a standard Kramers-Kronig identity. Defining $\delta\Omega_{M,\text{opt}} \equiv \frac{k_{\text{opt}}}{2m_{\text{eff}}\Omega_M}$, one finds:

$$\delta\Omega_{M,\text{opt}} = \frac{x_{\text{ZPF}}^2}{\hbar^2} \int_{-\infty}^{\infty} \frac{d\omega}{2\pi} S_{FF}[\omega] \left[\frac{1}{\Omega_M - \omega} - \frac{1}{\Omega_M + \omega} \right] \quad (2.31)$$

Thus, a knowledge of the quantum noise spectral density $S_{FF}[\omega]$ allows one to immediately extract both the optical spring coefficient, as well as the optical damping rate.

We now turn to the effects of the fluctuations in the radiation pressure force, and the effective temperature T_{rad} which characterizes them. This too can be directly related to $S_{FF}[\omega]$. Perhaps the most elegant manner to derive this is to perturbatively integrate out the dynamics of the cavity [24, 25]; this approach also has the benefit of going beyond simplest lowest-order-perturbation theory. One finds that the mechanical resonator is described by a *classical* Langevin equation of the form:

$$m\ddot{x}(t) = -(k + k_{\text{opt}})x(t) - m\Gamma_{\text{opt}}\dot{x}(t) + \xi_{\text{rad}}(t). \quad (2.32)$$

The optomechanical damping Γ_{opt} and optical spring k_{opt} are given respectively by Eqs. (2.25) and (2.31), except that one should make the replacement $\Omega_M \rightarrow \Omega'_M \equiv \Omega_M + \delta\Omega_{M,\text{opt}}$ in these equations. The last term $\xi_{\text{rad}}(t)$ above represents the fluctuating backaction force associated with photon number fluctuations in the cavity. Within our approximations of weak optomechanical coupling and weak intrinsic mechanical damping, this random force is Gaussian white noise, and is fully described by the spectral density:

$$S_{\xi_{\text{rad}}\xi_{\text{rad}}}[\omega] = m\Gamma_{\text{opt}} \coth(\hbar\Omega'_M/2k_B T_{\text{rad}}) = m\Gamma_{\text{opt}} (1 + 2\bar{n}_{\text{rad}}). \quad (2.33)$$

Here, T_{rad} is the effective temperature of the cavity backaction, and \bar{n}_{rad} is the corresponding number of thermal oscillator quanta. These quantities are determined by $S_{FF}[\omega]$ via:

$$1 + 2\bar{n}_{\text{rad}} \equiv \frac{S_{FF}[\Omega'_M] + S_{FF}[-\Omega'_M]}{S_{FF}[\Omega'_M] - S_{FF}[-\Omega'_M]} \quad (2.34)$$

Note that as the driven cavity is not in thermal equilibrium, T_{rad} will in general depend on the value of Ω_M ; a more detailed discussion of the concept of an effective temperature is given in Ref. [24].

Turning to the stationary state of the oscillator, we note that Eq. (2.32) is identical to the Langevin equation for an oscillator coupled to a thermal equilibrium bath at temperature T_{rad} . It thus follows that the stationary state of the oscillator will be a thermal equilibrium state at a temperature T_{rad} , and with an average number of quanta \bar{n}_{rad} . As far as the oscillator is concerned, T_{rad} is indistinguishable from a true thermodynamic bath temperature, even though the driven cavity is not itself in thermal equilibrium.

The more realistic case is of course where we include the intrinsic damping and heating of the mechanical resonator; even here, a similar picture holds. The intrinsic dissipation can be simply accounted for by adding to the RHS of Eq. (2.32) a damping term describing the intrinsic damping (rate, Γ_M), as well as a stochastic force term corresponding to the fridge temperature T . The resulting Langevin equation still continues to have the form of an oscillator coupled to a single equilibrium bath, where the total damping rate due to the bath is $\Gamma_M + \Gamma_{\text{opt}}$, and the effective temperature T_{eff} of the bath is determined by:

$$n_{\text{eff}} = \frac{\Gamma_M n_0 + \Gamma_{\text{opt}} \bar{n}_{\text{rad}}}{\Gamma_M + \Gamma_{\text{opt}}} \quad (2.35)$$

where n_0 is the Bose-Einstein factor corresponding to the bath temperature T :

$$n_0 = \frac{1}{\exp(\hbar\Omega'_M/k_B T) - 1} \quad (2.36)$$

We thus see that in the limit where $\Gamma_{\text{opt}} \gg \Gamma_M$, the effective mechanical temperature tends to the backaction temperature T_{rad} . This will be the lowest temperature possible via cavity cooling. Note that similar results may be obtained by using the Golden rule transition rates in Eq. (2.23) to formulate a master equation describing the probability $p_n(t)$ that the oscillator has n quanta at time t (see Sect. II B of Ref. [24]).

Before proceeding, it is worth emphasizing that the above results all rely on the total mechanical bandwidth $\Gamma_M + \Gamma_{\text{opt}}$ being sufficiently small that one can ignore the variance of $S_{FF}[\omega]$ across the mechanical resonance. When this condition is not satisfied, one can still describe backaction effects using the quantum noise approach,

with a Langevin equation similar to Eq. (2.32). However, one now must include the variation of $S_{FF}[\omega]$ with frequency; the result is that the optomechanical damping will not be purely local in time, and the stochastic part of the backaction force will not be white.

2.3.2 Application to the Standard Cavity Optomechanical Setup

The quantum noise approach to backaction is easily applied to the standard optomechanical cavity setup, where the backaction force operator \hat{F} is proportional to the cavity photon number operator. To calculate its quantum noise spectrum in the absence of any optomechanical coupling, we first write the equation of motion for the cavity annihilation operator \hat{a} in the Heisenberg picture, using standard input–output theory [26, 27]:

$$\frac{d}{dt}\hat{a} = (-i\omega_{\text{opt}} - \kappa/2)\hat{a} - \sqrt{\kappa}\hat{a}_{\text{in}}. \quad (2.37)$$

Here, \hat{a}_{in} describes the amplitude of drive laser, and can be decomposed as:

$$\hat{a}_{\text{in}} = e^{-i\omega_L t} (\bar{a}_{\text{in}} + \hat{d}_{\text{in}}), \quad (2.38)$$

where \bar{a}_{in} represents the classical amplitude of the drive laser (the input power is given by $P_{\text{in}} = \hbar\omega_{\text{opt}}|\bar{a}_{\text{in}}|^2$), and \hat{d}_{in} describes fluctuations in the laser drive. We consider the ideal case where these are vacuum noise, i.e. there is only shot noise in the incident laser drive, and no additional thermal or phase fluctuations. One thus finds that \hat{d}_{in} describes operator white noise:

$$\langle \hat{d}_{\text{in}}(t)\hat{d}_{\text{in}}^\dagger(t') \rangle = \langle [\hat{d}_{\text{in}}(t), \hat{d}_{\text{in}}^\dagger(t')] \rangle = \delta(t - t') \quad (2.39)$$

It is also useful to separate the cavity field operator into an average “classical” part and a quantum part,

$$\hat{a} = e^{-i\omega_L t} e^{i\phi} \left(\sqrt{\bar{n}_{\text{cav}}} + \hat{d} \right) \quad (2.40)$$

where $e^{i\phi}\sqrt{\bar{n}_{\text{cav}}}$ is the classical amplitude of the cavity field, and \hat{d} describes its fluctuations.

It is now straightforward to solve Eq. (2.37) for \hat{d} in terms of \hat{d}_{in} . As we will be interested in regimes where $\bar{n}_{\text{cav}} \gg 1$, we can focus on the leading-order-in- \bar{n}_{cav} term in the backaction force operator F :

$$\hat{F} \simeq \hbar G \sqrt{\bar{n}_{\text{cav}}} (\hat{d} + \hat{d}^\dagger) \quad (2.41)$$

Using this leading-order expression along with the solution for \hat{d}_{in} and Eq. (2.39), we find that the quantum noise spectral density $S_{FF}[\omega]$ (as defined in Eq. (2.21)) is given by:

$$S_{FF}[\omega] = \hbar^2 G^2 \bar{n}_{\text{cav}} \frac{\kappa}{(\omega + \Delta)^2 + (\kappa/2)^2} \quad (2.42)$$

$S_{FF}[\omega]$ is a simple Lorentzian, reflecting the cavity's density of states, and is centred at $\omega = -\Delta$, precisely the energy required to bring a drive photon onto resonance. The form of $S_{FF}[\omega]$ describes the final density of states for a Raman process where an incident drive photon gains ($\omega > 0$, anti-Stokes) or loses ($\omega < 0$, Stokes) a quanta $\hbar|\omega|$ of energy before attempting to enter the cavity. From Eq. (2.25), we can immediately obtain an expression for the optomechanical damping rate; it will be large if can make the density states associated with the anti-Stokes process at frequency Ω'_M much larger than that of the Stokes process at the same frequency. The optical spring coefficient also follows from Eq. (2.31).

We finally turn to \bar{n}_{rad} , the effective temperature of the backaction (expressed as a number of oscillator quanta). Using Eqs. (2.34) and (2.42), we find:

$$\bar{n}_{\text{rad}} = -\frac{(\Omega'_M + \Delta)^2 + (\kappa/2)^2}{4\Omega'_M \Delta} \quad (2.43)$$

As discussed, \bar{n}_{rad} represents the lowest possible temperature we can cool our mechanical resonator to. As a function of drive detuning Δ , \bar{n}_{rad} achieves a minimum value of

$$\bar{n}_{\text{rad}} \Big|_{\text{min}} = \left(\frac{\kappa}{4\Omega'_M} \right)^2 \frac{2}{1 + \sqrt{1 + (\kappa^2/4\Omega_M'^2)}} \quad (2.44)$$

for an optimal detuning of

$$\Delta = -\sqrt{\Omega_M'^2 + \kappa^2/4}. \quad (2.45)$$

We thus see that if one is in the so-called good cavity limit $\Omega_M \gg \kappa$, and if the detuning is optimized, one can potentially cool the mechanical resonator close to its ground state. In this limit, the anti-Stokes process is on-resonance, while the Stokes process is far off-resonance and hence greatly suppressed. The fact that the effective temperature is small but non-zero in this limit reflects the small but non-zero probability for the Stokes process, due to the Lorentzian tail of the cavity density of states. In the opposite, “bad cavity” limit where $\Omega_M \ll \kappa$, we see that the minimum of \bar{n}_{rad} tends to $\kappa/\Omega_M \gg 1$, while the optimal detuning tends to $\kappa/2$ (as anticipated in the semiclassical approach).

Note that the above results are easily extended to the case where the cavity is driven by thermal noise corresponding to a thermal number of cavity photons $n_{\text{cav},T}$. For a drive detuning of $\Delta = -\Omega_M$ (which is optimal in the good cavity limit), one

now finds that the \bar{n}_{rad} is given by [6]:

$$\bar{n}_{\text{rad}} = \left(\frac{\kappa}{4\Omega_M} \right)^2 + n_{\text{cav},T} \left(1 + 2 \left(\frac{\kappa}{4\Omega_M} \right)^2 \right) \quad (2.46)$$

As expected, one cannot backaction-cool a mechanical resonator to a temperature lower than that of the cavity.

2.3.3 Results for a Dissipative Optomechanical Coupling

A key advantage of the quantum noise approach is that it can be easily applied to alternate forms of optomechanical coupling. For example, it is possible have systems where the mechanical resonator modulates both the cavity frequency as well as the damping rate κ of the optical cavity [28, 29]. The position of the mechanical resonator will now couple to both the cavity photon number (as in the standard setup), as well as to the “photon tunnelling” term which describes the coupling of the cavity mode to the extra-cavity modes that damp and drive it. Because of these two couplings, the form of the effective backaction force operator \hat{F} is now modified from the standard setup. Nonetheless, one can still go ahead and calculate the optomechanical backaction using the quantum noise approach. In the simple case where the cavity is overcoupled (and hence its κ is due entirely to the coupling to the port used to drive it), one finds that the cavity’s backaction quantum force noise spectrum is given by [30, 31]:

$$S_{FF}[\omega] = \left(\frac{G_\kappa^2 \bar{n}_{\text{cav}}}{4\kappa} \right) \frac{\left[\omega + 2\Delta - \frac{2G}{G_\kappa} \kappa \right]^2}{(\omega + \Delta)^2 + \kappa^2/4} \quad (2.47)$$

Here, $G = -d\omega_{\text{opt}}/dx$ is the standard optomechanical coupling, while $G_\kappa = d\kappa/dx$ represents the dissipative optomechanical coupling. For $G_\kappa = 0$, we recover the Lorentzian spectrum of the standard optomechanical setup given in Eq. (2.42) whereas for $G_\kappa \neq 0$, $S_{FF}[\omega]$ has the general form of a Fano resonance. Such lineshapes arise as the result of interference between resonant and non-resonant processes; here, the resonant channel corresponds to fluctuations in the cavity amplitude, whereas the non-resonant channel corresponds to the incident shot noise fluctuations on the cavity. These fluctuations can interfere destructively, resulting in $S_{FF}[\omega] = 0$ at the special frequency $\omega = -2\Delta + 2G/G_\kappa$. If one tunes Δ such that this frequency coincides with $-\Omega_M$, it follows immediately from Eq. (2.34) that the cavity backaction has an effective temperature of zero, and can be used to cool the mechanical resonator to its ground state. This special detuning causes the destructive interference to completely suppress the probability of the cavity backaction exciting the mechanical resonator, whereas the opposite process of absorption is not suppressed. This “interference cooling” does not require one to be in the good cavity limit, and thus could be potentially useful for the cooling of low-frequency (relative

to κ) mechanical modes. However, the presence of internal loss in the cavity places limits on this technique, as it suppresses the perfect destructive interference between resonant and non-resonant fluctuations [30, 31].

References

1. C.K. Law, Phys. Rev. A **51**, 2537 (1995)
2. M. Aspelmeyer, T.J. Kippenberg, F. Marquardt (2013), [arXiv:1303.0733](https://arxiv.org/abs/1303.0733)
3. V.B. Braginsky, A.B. Manukin, Sov. Phys. JETP **25**, 653 (1967)
4. A. Dorsel, J.D. McCullen, P. Meystre, E. Vignes, H. Walther, Phys. Rev. Lett. **51**, 1550 (1983)
5. F. Marquardt, J.P. Chen, A.A. Clerk, S.M. Girvin, Phys. Rev. Lett. **99**, 093902 (2007)
6. J. Dobrindt, I. Wilson-Rae, T.J. Kippenberg, Phys. Rev. Lett. **101**(26), 263602 (2008)
7. S. Groblacher, K. Hammerer, M.R. Vanner, M. Aspelmeyer, Nature **460**, 724 (2009)
8. G.S. Agarwal, S. Huang, Phys. Rev. A **81**, 041803 (2010)
9. S. Weis, R. Rivière, S. Deléglise, E. Gavartin, O. Arcizet, A. Schliesser, T.J. Kippenberg, Science **330**, 1520 (2010)
10. F. Marquardt, J.G.E. Harris, S.M. Girvin, Phys. Rev. Lett. **96**, 103901 (2006)
11. M. Ludwig, B. Kubala, F. Marquardt, New J. Phys. **10**, 095013 (2008)
12. H. Rokhsari, T.J. Kippenberg, T. Carmon, K. Vahala, Opt. Express **13**, 5293 (2005)
13. T. Carmon, H. Rokhsari, L. Yang, T.J. Kippenberg, K.J. Vahala, Phys. Rev. Lett. **94**, 223902 (2005)
14. T.J. Kippenberg, H. Rokhsari, T. Carmon, A. Scherer, K.J. Vahala, Phys. Rev. Lett. **95**, 033901 (2005)
15. C. Höhberger, K. Karrai, in *Nanotechnology 2004*, Proceedings of the 4th IEEE conference on nanotechnology (2004), p. 419
16. C. Metzger, M. Ludwig, C. Neuenhahn, A. Ortlieb, I. Favero, K. Karrai, F. Marquardt, Phys. Rev. Lett. **101**, 133903 (2008)
17. G. Heinrich, M. Ludwig, J. Qian, B. Kubala, F. Marquardt, Phys. Rev. Lett. **107**, 043603 (2011)
18. C.A. Holmes, C.P. Meaney, G.J. Milburn, Phys. Rev. E **85**, 066203 (2012)
19. M. Zhang, G. Wiederhecker, S. Manipatruni, A. Barnard, P.L. McEuen, M. Lipson, Phys. Rev. Lett. **109**, 233906 (2012)
20. M. Bagheri, M. Poot, L. Fan, F. Marquardt, H.X. Tang, Phys. Rev. Lett. **111**, 213902 (2013)
21. T. Carmon, M.C. Cross, K.J. Vahala, Phys. Rev. Lett. **98**, 167203 (2007)
22. I. Wilson-Rae, N. Nooshi, W. Zwerger, T.J. Kippenberg, Phys. Rev. Lett. **99**, 093901 (2007)
23. C. Genes, D. Vitali, P. Tombesi, S. Gigan, M. Aspelmeyer, Phys. Rev. A **77**, 033804 (2008)
24. A.A. Clerk, M.H. Devoret, S.M. Girvin, F. Marquardt, R.J. Schoelkopf, Rev. Mod. Phys. **82**, 1155 (2010)
25. J. Schwinger, J. Math. Phys. **2**, 407 (1961)
26. C.W. Gardiner, M.J. Collett, Phys. Rev. A **31**(6), 3761 (1985)
27. C.W. Gardiner, P. Zoller, *Quant. Noise* (Springer, Berlin, 2000)
28. M. Li, W.H.P. Pernice, H.X. Tang, Phys. Rev. Lett. **103**(22), 223901 (2009)
29. J.C. Sankey, C. Yang, B.M. Zwickl, A.M. Jayich, J.G.E. Harris, Nat. Phys. **6**, 707 (2010)
30. F. Elste, S.M. Girvin, A.A. Clerk, Phys. Rev. Lett. **102**, 207209 (2009)
31. F. Elste, A.A. Clerk, S.M. Girvin, Phys. Rev. Lett. **103**, 149902(E) (2009)

Cavity Optomechanics

Nano- and Micromechanical Resonators Interacting with
Light

Aspelmeyer, M.; Kippenberg, T.J.; Marquardt, F. (Eds.)

2014, VIII, 357 p. 133 illus., 93 illus. in color., Hardcover

ISBN: 978-3-642-55311-0